nature portfolio

https://doi.org/10.1038/s41596-021-00546-w

Supplementary information

RNA-extraction-free nano-amplified colorimetric test for point-of-care clinical diagnosis of COVID-19

In the format provided by the authors and unedited

Supplementary information

RNA Extraction-Free Nano-Amplified Colorimetric Test for Point-of-Care Clinical Diagnosis of COVID-19

Maha Alafeef,[†,a,b,c] Parikshit Moitra,[†,c] Ketan Dighe[†,c,d] and Dipanjan Pan*[,a,c,d]

[a] Department of Bioengineering, University of Illinois at Urbana-Champaign, Urbana, Illinois 61801, United States.

[b] Biomedical Engineering Department, Jordan University of Science and Technology, Irbid 22110, Jordan.

[c] Departments of Diagnostic Radiology and Nuclear Medicine and Pediatrics, Center for Blood Oxygen Transport and Hemostasis, University of Maryland Baltimore School of Medicine, Baltimore, Maryland 21201, United States.

[d] Department of Chemical, Biochemical and Environmental Engineering, University of Maryland, Baltimore County, Baltimore, Maryland 21250, United States.

* Correspondence: dipanjan@som.umaryland.edu

[†] Equal contribution

Supplementary discussion

1. Biological Materials

- Vero cells infected with COVID-19 causative virus, SARS-CoV-2
- Vero cells infected with MERS-CoV

2. Trial runs and Optimization steps.

Multiple trial runs were performed to optimize the protocol to achieve the optimum results. These steps are illustrated below:

(i) During the preparation of citrate stabilized AuNPs, the $HAuCl_4$ solution was first heated to boil, sodium citrate solution was added to the mixture and stirred for an additional 10 mins where the color of the mixture changed from yellow to pink[1]. If the reaction mixture was stirred for more time, the color of the solution changed towards purple indicating the formation of larger size of gold nanoparticles[2-4]. As our detection principle lies on the formation of agglomerated AuNPs, we tried to optimize the sensing protocol with larger size of AuNPs. But we did not observe a distinct change in color of the solution in presence of target amplified genetic material when larger size of Au-ASO nanoparticles were used for the sensing purpose. Accordingly, we have tested our protocol with several size of AuNPs and optimized the NACT method with 10 nm of AuNPs where we observed the distinct change in color from pink to purple in presence of amplified target gene.

(ii) First citrate stabilized AuNPs were prepared with a concentration of ~3×10^{10} particle/mL[3]. Two of the ASOs were then added separately at three different concentrations of 0.5, 1, and 2 μM, respectively. This mixture was then stirred at room temperature (25 ± 1 °C) for 30 mins. The uncapped ASOs were then removed from the solution by centrifugation at 20 000 rcf for 15 min. The residual pellet was resuspended in an equivalent volume of water. Thus, 6 separate samples were prepared from the two ASOs at three different concentrations[3]. These particles are named as Au-ASOxL, Au-ASOxM and Au-ASOxH where x represents the number of ASO (1 or 2) and L, M, and H are indicative of low (0.5 μM), medium (1 μM), and high (2 μM) concentrations of ASOs respectively. These nanoparticles were kept at 4 °C for future use. A QuantiFluor ssDNA system (Promega Corporation) was used to quantify the number of ASO conjugated to each gold nanoparticle[3,5]. It was realized that Au-ASO1M and Au-ASO2L is the optimum choice for this NACT method where the used concentration of ASO1 is 5 μM and ASO2 is 2.5 μM. This optimization has been carried out by monitoring the relative agglomeration of the respective ASO-capped AuNPs in presence of their

target gene as monitored from UV-Visible absorbance spectroscopy. A detailed study has been published recently from our group.[3,6,7]

(iii) It was realized that NAA time can be extended as necessary to target very low viral copy numbers. Accordingly, we have tested our protocol at several incubation time points, *e.g.* 30 mins and 45 mins. But optimum results with minimal false-positive signals were observed when the incubation time was kept fixed at 30 mins. Agarose gel electrophoresis also proved the successful amplification of the nucleic acids over this period in presence of the NAA primers (Fig. 5).

(iv) We have also tested our NAA protocol without the addition of the loop primers. But it was observed that only the addition of inner and outer primers during the NAA reaction increased the false-positive signals. The addition of loop primers greatly improved the performance of the test[8].

(v) Increase in false-positive signals was also found when the NAA mixture was tested with Au-ASO formulation directly after the amplification period of 30 mins. But if the mixture, after the required NAA period, was heated to > 80°C for 5 minutes to inactivate *Bst* 2.0 polymerase and reverse transcriptase, the false-positive signals reduce largely.

(vi) The amplified inactivated NA mixture was then treated with Au-ASO formulations having an equivalent mixture of Au-ASO1 and Au-ASO2. It was understood that NAA produced cDNA strands from RNA strand during this period. Therefore, the cDNA strand must be unfolded to a single strand during its binding with ASOs[9]. Accordingly, we first added Au-ASO formulation to the deactivated NAA mixture at room temperature and then heated the mixture at 65 °C to unfold the cDNA duplex strand to a single strand so that it can react efficiently and effectively with the ASO strands leading to the agglomeration of AuNPs. This incubation time was further optimized to be ~5 mins where we observed the maximum diagnosis efficiency and minimal false-positive signals from our NACT method.

(vii) We have used SARS-CoV-2 genomic RNA (NR 52347, BEI resources) to evaluate the limit of detection (LOD) of our NACT methodology. NR-52347 contains a preparation of genomic RNA extracted from heat-inactivated severe acute respiratory syndrome-related coronavirus 2 (SARS-CoV-2), isolate USA-WA1/2020 in the buffer, for use as a positive control in qPCR assays. Towards this, nucleic acid was extracted from a preparation of heat-inactivated SARS-CoV-2, isolate USA-WA-1/2020 (BEI Resources NR-52286 lot 70033321) using a QIAamp® Viral RNA Mini Kit (Qiagen® 52906) and vialed in TE buffer (10 mM Tris-HCl, 1 mM EDTA, pH 8.0). Several samples with various copy numbers ranging from $5x10^7$ copies/µl to 1 copies/ml were used to evaluate the test. The lowest

detectable RNA concentration which is distinguishable from the response of the negative samples represents the LOD of the test which is found to be 10 copies/μL for our test.

We have tested the performance of the protocol using de-identified clinical samples collected from patients and spiked viral RNA samples in artificial saliva. In order to evaluate the effectiveness of our diagnostic test, we have first tested our assay with RNA samples extracted from the clinical swabs. Further to this, we have investigated our sensor's efficiency in an RNA-extraction-free approach using 22 clinical samples directly. We have summarized the results in Table 4. The cycle threshold (Ct) values of the clinical samples were used in evaluating the performance of the RNA-extraction-free kit (Fig. 8). The confusion matrix from the results was also added to the supplementary data in Supplementary Fig. 3. The evaluation of our protocol using clinical samples was conducted using randomly obtained COVID-19 positive and negative samples. The cycle threshold (Ct) number of the clinical samples, used in this study and as measured from the RT-qPCR analyses, are ranging from 13-29. In this range of Ct numbers, the test results are independent of the sample Ct numbers. Evaluation of the test results beyond this Ct number requires further experiments.

3. Validations and Controls.

The NACT method has been validated with RT-PCR test results and the statistical significance of the methods has also been evaluated[6,7]. The visual 'naked-eye' color of the test results was also validated from the change in the surface plasmon band of the gold nanoparticles arising due to their agglomeration in presence of the target genetic sequence.

Supplementary Data 1

N-gene sequence.

Target gene sequence of severe acute respiratory syndrome coronavirus 2 isolate 2019- nCoV/USA-WA1-A12/2020 gene="N" (1260 number of nucleotide bases) Accession MT020880 CDS 28274..29533 /product="nucleocapsid phosphoprotein" /protein_id="QHU79201.1" /translation="MSDNGPQNQRNAPRITFGGPSDSTGSNQNGERSGARSKQRRPQG

LPNNTASWFTALTQHGKEDLKFPRGQGVPINTNSSPDDQIGYYRRATRRIRGGDGKMK

DLSPRWYFYYLGTGPEAGLPYGANKDGIIWVATEGALNTPKDHIGTRNPANNAAIVLQ

LPQGTTLPKGFYAEGSRGGSQASSRSSSRSRNSSRNSTPGSSRGTSPARMAGNGGDAA

LALLLLDRLNQLESKMSGKGQQQQGQTVTKKSAAEASKKPRQKRTATKAYNVTQAFGR

RGPEQTQGNFGDQELIRQGTDYKHWPQIAQFAPSASAFFGMSRIGMEVTPSGTWLTYT

GAIKLDDKDPNFKDQVILLNKHIDAYKTFPPTEPKKDKKKKADETQALPQRQKKQQTV

TLLPAADLDDFSKQLQQSMSSADSTQA”

28321 gtttggtgga ccctcagatt caactggcag taaccagaat ggagaacgca gtggggcgcg

28381 atcaaaacaa cgtcggcccc aaggtttacc caataatact gcgtcttggt tcaccgctct

28441 cactcaacat ggcaaggaag accttaaatt ccctcgagga caaggcgttc caattaacac

28501 caatagcagt ccagatgacc aaattggcta ctaccgaaga gctaccagac gaattcgtgg

28561 tggtgacggt aaaatgaaag atctcagtcc aagatggtat ttctactacc taggaactgg

28621 gccagaagct ggacttccct atggtgctaa caaagacggc atcatatggg ttgcaactga

28681 gggagccttg aatacaccaa aagatcacat tggcacccgc aatcctgcta acaatgctgc

28741 aatcgtgcta caacttcctc aaggaacaac attgccaaaa ggcttctacg cagaagggag

28801 cagaggcggc agtcaagcct cttctcgttc ctcatcacgt agtcgcaaca gttcaagaaa

28861 ttcaactcca ggcagcagta ggggaacttc tcctgctaga atggctggca atggcggtga

28921 tgctgctctt gctttgctgc tgcttgacag attgaaccag cttgagagca aaatgtctgg

28981 taaaggccaa caacaacaag gccaaactgt cactaagaaa tctgctgctg aggcttctaa

29041 gaagcctcgg caaaaacgta ctgccactaa agcatacaat gtaacacaag ctttcggcag

29101 acgtggtcca gaacaaaccc aaggaaattt tggggaccag gaactaatca gacaaggaac

29161 tgattacaaa cattggccgc aaattgcaca atttgccccc agcgcttcag cgttcttcgg

29221 aatgtcgcgc attggcatgg aagtcacacc ttcgggaacg tggttgacct acacaggtgc

29281 catcaaattg gatgacaaag atccaaattt caaagatcaa gtcattttgc tgaataagca

29341 tattgacgca tacaaaacat tcccaccaac agagcctaaa aaggacaaaa agaagaaggc

29401 tgatgaaact caagccttac cgcagagaca gaagaaacag caaactgtga ctcttcttcc

29461 tgctgcagat ttggatgatt tctccaaaca attgcaacaa tccatgagca gtgctgactc

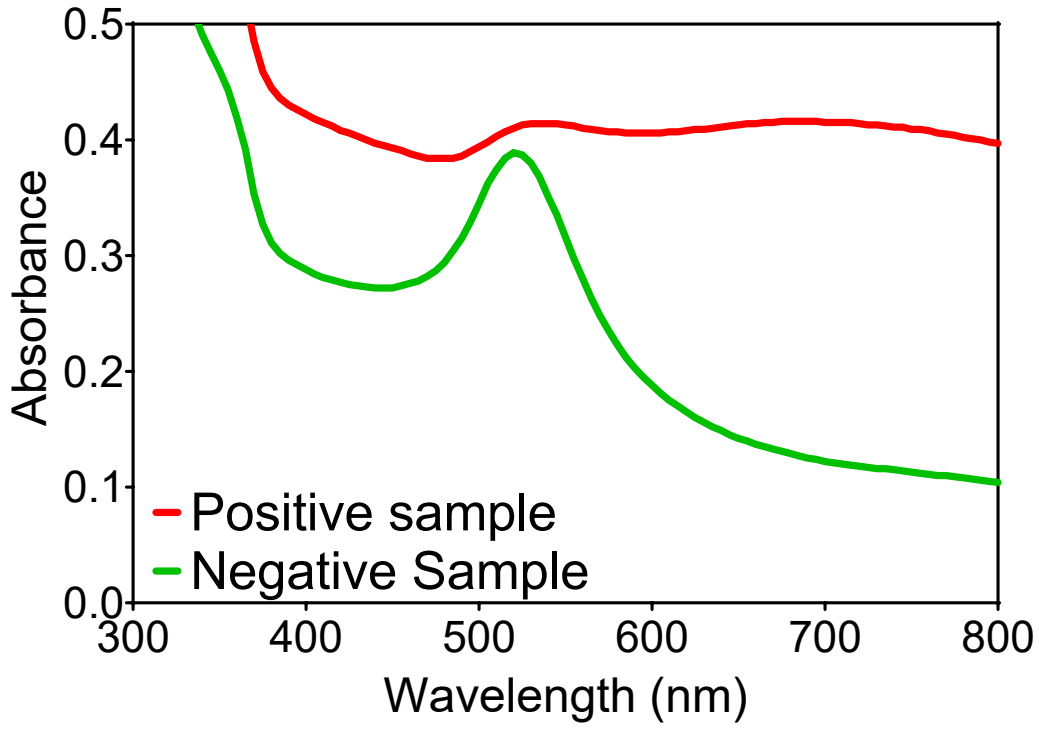

Supplementary Fig. 1 Aggregation of AuNPs confirmed using UV-vis spectroscopy. Absorption spectrum of the ASO-capped AuNPs measured using UV-Vis spectroscopy in the range of 300-800nm. The spectrum shows a response of the AuNPs to confirmed positive and negative COVID-19 samples tested using our protocol. A significant shift of the AuNPs plasmonic peak (~520) was observed in the presence of SARS-CoV-2 confirming the aggregation of the particles[6,7].

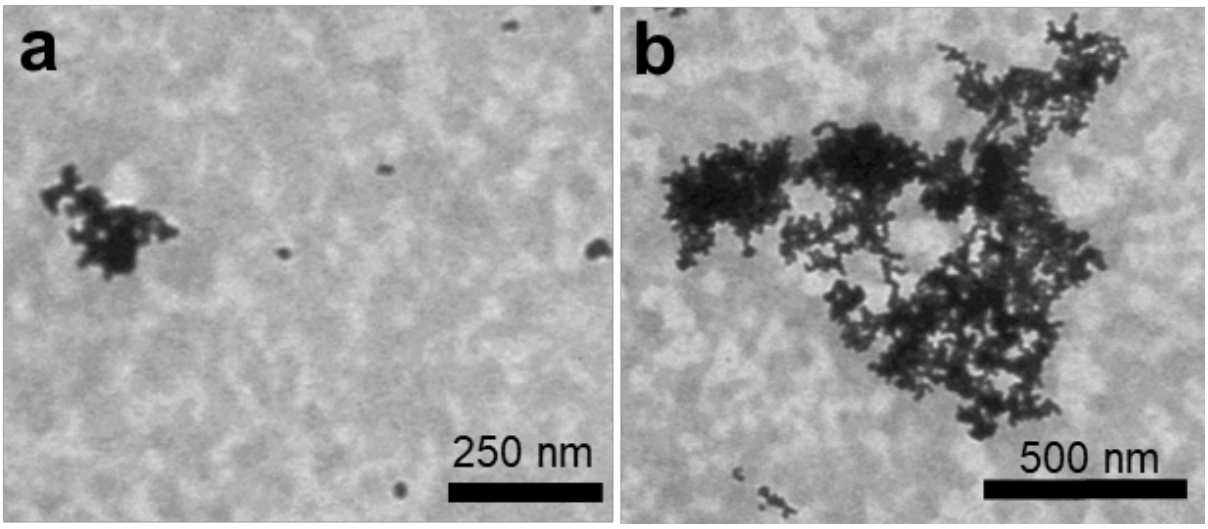

Supplementary Fig. 2 Aggregation of AuNPs confirmed using TEM. Transmission electron microscopy images of the AuNPs conjugated to ASOs in the presence of SARS-CoV-2 RNA. The gold nanoparticles form large aggregates with different sizes ranging from 80-120nm.

a

Our work	Diagnosis using RT-PCR: Positive	Diagnosis using RT-PCR: Negative
Positive	59	0
Negative	1	30

Accuracy: 98.9%, Sensitivity: 98.33%, Specificity: 100%

b

Our work	Diagnosis using RT-PCR: Positive	Diagnosis using RT-PCR: Negative
Positive	28	0
Negative	1	32

Accuracy=98.4%, Sensitivity=96.6%, Specificity=100%

Supplementary Fig. 3 Benchmarking the performance of the protocol. The results obtained using our protocol were benchmarked to the gold standard RT-qPCR as shown with their associated statistics including accuracy, sensitivity, and specificity. Confusion matrix of the protocol's results against those obtained by RT-qPCR using a) 90 samples of artificial saliva spiked with RNA from positive COVID-19 samples and Vero cells infected with SARS-CoV-2 (n=60), negative COVID-19 samples (n=21), and MERS-CoV (n=9). b) RNA extracted from 61 clinical samples[6,7]. As shown in the confusion matrix in a, only one sample has been misclassified as negative using our protocol. As shown in **b** the samples tested after the RNA isolation showed a misclassification of one COVID-19 positive sample which has been classified as negative using our test.

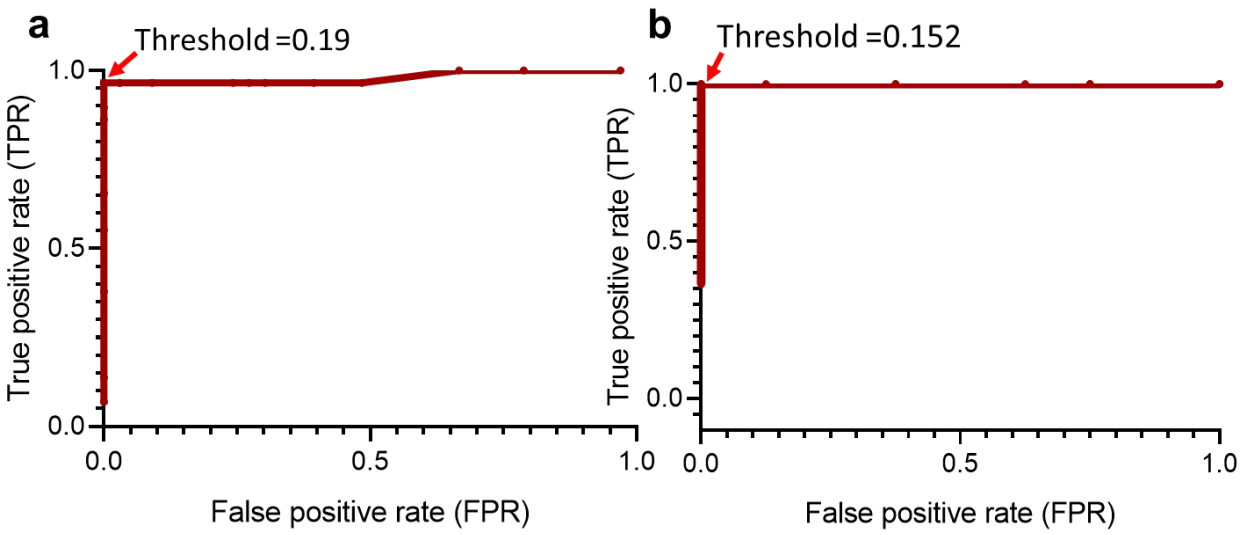

Supplementary Fig. 4 Receiver operating characteristic (ROC) curves of the NACT test. a) ROC curve corresponding to the data obtained from applying the protocol on RNA extracted samples. b) ROC curve corresponding to the data obtained from RNA-extraction free protocol. 22 different threshold values have been used to classify the results and assign a diagnosis to each sample. The associated true positive rate (TPR) and false-positive rate (FPR) have been calculated for each threshold value. The threshold value which both maximizes the TPR and minimizes the FPR has been selected.

Supplementary Table 1. Performance of the protocol with prior RNA extraction, evaluated during optimization of the RNA extraction-free protocol using artificial saliva samples spiked with purified RNA, and using clinical samples directly without RNA extraction.

Condition	Number of samples	Accuracy	Sensitivity	Specificity
RNA extracted from clinical samples	**61 samples** -29 positive -32 negative	98.4%	96.6%	100%
Artificial saliva samples spiked with purified RNA	**90 samples** -60 samples spiked with RNA from positive COVID-19 samples or Vero cells infected with SARS-CoV-2 -21 samples spiked with RNA from negative COVID-19 samples -9 samples spiked with RNA extracted from Vero cells infected with MERS-CoV	98.9%	98.33%	100%
Direct clinical samples	**22 samples** -11 positives -11 negatives	100%	100%	100%

The accuracy, sensitivity and specifcity values caluclated using the formulae given in the Software subsection in the Materials section.

Supplementary Table 2. Cost analysis of the NACT kit.*

Component	Material	Fraction used /reaction	Cost ($)/2000 reaction	Cost/reaction
NAA mixture	Warmstart Lamp Kit (DNA And RNA)	$5x\ 10^{-2}$	286.28	0.1431
NAA Primers	F3, B3, FIP, BIP, Loop forward primer, loop backward primer	$5x\ 10^{-2}$	2.88655	0.0014
Au-ASO	AuNPs raw materials include Hydrogen Tetrachloroaurate Sodium Citrate Tribasic Dihydrate. AuNPs conjugated to Thiolated antisense oligonucleotide 1&2	1	11.1	0.0056
		Total cost	**$300.267/2000 reactions**	**$0.1501/reaction**

*Cost analysis of the test for COVID-19 detection. Fraction used is calculated based on the required amount in 10µl final reaction mixture. Some reagents such as RNAse free water are omitted from the cost analysis because their contribution to the overall cost is negligible.

Supplementary Table 3. Timing estimates of the protocol steps.

Primary Stages	**Steps**	**Time Required**
Preparation of antisense oligonucleotide capped gold nanoparticles (Au-ASO) (Steps 1-7)	Synthesis of citrate stabilized gold nanoparticles	1 hour
	Preparation and purification of Au-ASO	1 hour
Collection of samples and used either directly or after RNA extraction and purification (Steps 8 & 9)	Direct sampling (Required step)	1 minute
	Extraction and purification of RNA (Optional step)	30 minutes
Isothermal amplification of the target genetic material (Steps 10-15)	Isothermal amplification of nucleic acids	30 minutes at 65 °C
	Inactivation of Bst 2.0 polymerase and reverse transcriptase	5 minutes at > 80 °C
Colorimetric detection of the target genetic material (Steps 16-17)	Colorimetric detection	5 minutes at 65 °C

Supplementary Table 4. Comparison of the current analytical performance of COVID-19 detection approaches.

Detection Approach	Target Analyte	Sample Source	Test Result Time (min)	LOD	Sensitivity (%)	Specificity (%)	Cost	Readout	Instrumentation	Ref
RT-PCR	Viral RNA	Respiratory swabs, saliva, sputum, bronchoalveolar lavage fluid	120 – 140	0.15 – 100 copy/ µL	90 – 100	100	$ 40 – 300	Fluorescence	Thermocycler High throughput; can be run in moderate/high complexity lab	10-14
Molecular POC	Viral RNA	Respiratory swabs	13 – 60	0.1 – 10 copy/ µL	> 95	100	$ 10 – 150	Fluorescence /Colorimetric	Minimal equipment (e.g., Heat Block) Medium throughput; can be run at POC near the patient	13
Biosensors (LFA/RDT)	Viral RNA/ Antigen/Antibody	Respiratory swabs, blood	< 60	0.2 pM	Limited data	Limited data	$ 0.5 – 5	Fluorescence /Colorimetric /Electrochemical	Minimal equipment Medium throughput; can be run at POC near the patient	6,13,15-19
ELISA	Antibody	Blood	60 – 180	N.A	86 – 100	89 – 100	$ 40 – 200	Fluorescence /Colorimetric	Plate reader High throughput; can be run in moderate/high complexity lab	13,18,20
CT – Computed tomography	Human Tissue (Lungs)	Radio contrast agents	<60	N.A	86 – 98	25	$ 270 – 5000	Computer-processed combinations of multiple X-ray measurements	CT scanner Low throughput; Can only be run in high complexity lab	13,21
CRISPR based approaches	Viral RNA	Respiratory swabs, saliva	45 – 70	2 – 10 copy/ µL	95 – 100	100	$ 4 – 40	Fluorescence /Colorimetric	Minimal equipment Medium throughput; Can be run in moderate complexity lab	13,22-24
NGS – Next generation sequencing	Viral RNA	Respiratory swabs, bronchoalveolar lavage fluid	1 – 2 days	N.A	96.98%	99.99%	Varies – depends on technology	Digital readout	Sequencer High throughput; Can only be run in high complexity lab	25,26
NACT	Viral RNA	Respiratory swabs	<60	10 copies/ µL	>96.6	100	$0.1501/reaction	Colorimetric	Minimal instrumentation. Example: Heat block	Current work

N.A: not applicable (the information are not available)

Supplementary Table 5. Details of the sample preparation protocols used for direct sampling.

Condition no.	**Description of the protocol**	**Results**	**Photographic images of the tubes**
GITC lysis buffer condition #1	Add guanidinium isothiocyanate solution (GITC lysis buffer) to the sample and water in a sample: lysis buffer: water ratio of 2:2:1	TP=1 TN=2 FP=0 FN=1	
GITC lysis buffer condition # 2	Add guanidine isothiocyanate solution (GITC lysis buffer) to sample and water in a sample: lysis buffer: water ratio of 2:1:2	TP=2 TN=2 FP=0 FN=0	
Tween-20 lysis buffer condition #1	Add 10% v/v of tween-20 to sample and water in a sample: lysis buffer: water ratio of 2:2:1	TP=0 TN=2 FP=0 FN=2	
Tween-20 lysis buffer condition #2	Add 10% v/v of tween-20 to sample and water in a sample: lysis buffer: water ratio of 2:1:2	TP=0 TN=2 FP=0 FN=2	

HUDSON	Heat to 95°C for 5 min followed by immediate incubation over ice	TP=1 TN=2 FP=0 FN=1	

These treatment conditions involved HUDSON (heating unextracted diagnostic samples to obliterate nucleases) that includes incubation of the sample at 95 °C for 5 mins. This includes heating the sample, rupturing the outer membrane of the virus to release the enclosed nucleic acid[27,28]. Alternatively, the viral membrane can be ruptured by the treatment of lysis buffer either containing tween-20 or guanidium isothiocyanate (GITC) at two different ratios for a definite incubation period. GITC lysis buffer condition # 2 found to be the best among other tested methods.

References

1 Kumar, K., Moitra, P., Bashir, M., Kondaiah, P. & Bhattacharya, S. Natural tripeptide capped pH-sensitive gold nanoparticles for efficacious doxorubicin delivery both in vitro and in vivo. *Nanoscale* **12**, 1067-1074, doi:10.1039/C9NR08475D (2020).

2 Chegel, V. *et al.* Gold Nanoparticles Aggregation: Drastic Effect of Cooperative Functionalities in a Single Molecular Conjugate. *The Journal of Physical Chemistry C* **116**, 2683-2690, doi:10.1021/jp209251y (2012).

3 Moitra, P. *et al.* Rapid and Low-cost Sampling for Detection of Airborne SARS-CoV-2 in Dehumidifier Condensate. *medRxiv*, 2020.2010.2008.20208785, doi:10.1101/2020.10.08.20208785 (2020).

4 Misra, S. K. *et al.* In situ plasmonic generation in functional ionic-gold-nanogel scaffold for rapid quantitative bio-sensing. *Biosensors and Bioelectronics* **120**, 77-84, doi:https://doi.org/10.1016/j.bios.2018.08.019 (2018).

5 Alafeef, M., Fraiwan, M., Alkhalaf, H. & Audat, Z. Shannon entropy and fuzzy C-means weighting for AI-based diagnosis of vertebral column diseases. *Journal of Ambient Intelligence and Humanized Computing* **11**, 2557-2566, doi:10.1007/s12652-019-01312-3 (2020).

6 Alafeef, M., Dighe, K., Moitra, P. & Pan, D. Rapid, Ultrasensitive, and Quantitative Detection of SARS-CoV-2 Using Antisense Oligonucleotides Directed Electrochemical Biosensor Chip. *ACS Nano* **14**, 17028-17045, doi:10.1021/acsnano.0c06392 (2020).

7 Moitra, P., Alafeef, M., Dighe, K., Frieman, M. B. & Pan, D. Selective Naked-Eye Detection of SARS-CoV-2 Mediated by N Gene Targeted Antisense Oligonucleotide Capped Plasmonic Nanoparticles. *ACS Nano* **14**, 7617-7627, doi:10.1021/acsnano.0c03822 (2020).

8 Ding, X. *et al.* Improved detection limit in rapid detection of human enterovirus 71 and coxsackievirus A16 by a novel reverse transcription-isothermal multiple-self-matching-initiated amplification assay. *J Clin Microbiol* **52**, 1862-1870, doi:10.1128/JCM.03298-13 (2014).

9 Hüttemann, M. Partial heat denaturation step during reverse transcription and PCR screening yields full-length 5'-cDNAs. *BioTechniques* **32**, 730, 732, 734, 736, doi:10.2144/02324bm02 (2002).

10 Corman, V. M. *et al.* Detection of 2019 novel coronavirus (2019-nCoV) by real-time RT-PCR. *Euro surveillance : bulletin Europeen sur les maladies transmissibles = European communicable disease bulletin* **25**, 2000045, doi:10.2807/1560-7917.ES.2020.25.3.2000045 (2020).

11 Vogels, C. B. F. *et al.* Analytical sensitivity and efficiency comparisons of SARS-CoV-2 RT–qPCR primer–probe sets. *Nature Microbiology* **5**, 1299-1305, doi:10.1038/s41564-020-0761-6 (2020).

12 Xue, G. *et al.* Reverse-Transcription Recombinase-Aided Amplification Assay for Rapid Detection of the 2019 Novel Coronavirus (SARS-CoV-2). *Analytical Chemistry* **92**, 9699-9705, doi:10.1021/acs.analchem.0c01032 (2020).

13 Carter, L. J. *et al.* Assay Techniques and Test Development for COVID-19 Diagnosis. *ACS Central Science* **6**, 591-605, doi:10.1021/acscentsci.0c00501 (2020).

14 Udugama, B. *et al.* Diagnosing COVID-19: The Disease and Tools for Detection. *ACS Nano* **14**, 3822-3835, doi:10.1021/acsnano.0c02624 (2020).

15 Qiu, G. *et al.* Dual-Functional Plasmonic Photothermal Biosensors for Highly Accurate Severe Acute Respiratory Syndrome Coronavirus 2 Detection. *ACS Nano* **14**, 5268-5277, doi:10.1021/acsnano.0c02439 (2020).

16 Seo, G. *et al.* Rapid Detection of COVID-19 Causative Virus (SARS-CoV-2) in Human Nasopharyngeal Swab Specimens Using Field-Effect Transistor-Based Biosensor. *ACS Nano* **14**, 5135-5142, doi:10.1021/acsnano.0c02823 (2020).
17 Krüttgen, A. *et al.* Comparison of four new commercial serologic assays for determination of SARS-CoV-2 IgG. *Journal of Clinical Virology* **128**, 104394, doi:https://doi.org/10.1016/j.jcv.2020.104394 (2020).
18 Lassaunière, R. *et al.* Evaluation of nine commercial SARS-CoV-2 immunoassays. *medRxiv*, 2020.2004.2009.20056325, doi:10.1101/2020.04.09.20056325 (2020).
19 Ventura, B. D. *et al.* Colorimetric Test for Fast Detection of SARS-CoV-2 in Nasal and Throat Swabs. *ACS Sensors* **5**, 3043-3048, doi:10.1021/acssensors.0c01742 (2020).
20 Espejo, A. P. *et al.* Review of Current Advances in Serologic Testing for COVID-19. *Am J Clin Pathol* **154**, 293-304, doi:10.1093/ajcp/aqaa112 (2020).
21 Ai, T. *et al.* Correlation of Chest CT and RT-PCR Testing for Coronavirus Disease 2019 (COVID-19) in China: A Report of 1014 Cases. *Radiology* **296**, E32-E40, doi:10.1148/radiol.2020200642 (2020).
22 Broughton, J. P. *et al.* CRISPR–Cas12-based detection of SARS-CoV-2. *Nature Biotechnology* **38**, 870-874, doi:10.1038/s41587-020-0513-4 (2020).
23 Hou, T. *et al.* Development and Evaluation of A CRISPR-based Diagnostic For 2019-novel Coronavirus. *medRxiv*, 2020.2002.2022.20025460, doi:10.1101/2020.02.22.20025460 (2020).
24 Joung, J. *et al.* Point-of-care testing for COVID-19 using SHERLOCK diagnostics. *medRxiv*, 2020.2005.2004.20091231, doi:10.1101/2020.05.04.20091231 (2020).
25 Huang, J. & Zhao, L. A high-throughput strategy for COVID-19 testing based on next-generation sequencing. *medRxiv*, 2020.2006.2012.20129718, doi:10.1101/2020.06.12.20129718 (2020).
26 Lih, C.-J. *et al.* Analytical Validation of the Next-Generation Sequencing Assay for a Nationwide Signal-Finding Clinical Trial: Molecular Analysis for Therapy Choice Clinical Trial. *The Journal of molecular diagnostics : JMD* **19**, 313-327, doi:10.1016/j.jmoldx.2016.10.007 (2017).
27 Kellner, M. J., Koob, J. G., Gootenberg, J. S., Abudayyeh, O. O. & Zhang, F. SHERLOCK: nucleic acid detection with CRISPR nucleases. *Nat Protoc* **14**, 2986-3012, doi:10.1038/s41596-019-0210-2 (2019).
28 Myhrvold, C. *et al.* Field-deployable viral diagnostics using CRISPR-Cas13. *Science* **360**, 444-448, doi:10.1126/science.aas8836 (2018).